

## CONTRIBUTION OF THE ODIN SPACE TELESCOPE TO THE UNDERSTANDING OF THE ORIGIN OF WATER VAPOR IN THE ATMOSPHERE OF JUPITER

T. Cavalié<sup>1</sup>, F. Billebaud<sup>2</sup>, E. Lellouch<sup>3</sup>, N. Biver<sup>4</sup>, M. Dobrijevic<sup>5</sup>, J. Brillet<sup>6</sup>, A. Lecacheux<sup>7</sup>, Å. Hjalmarson<sup>8</sup>, A. Sandqvist<sup>9</sup>, U. Frisk<sup>10</sup>, M. Olberg<sup>11</sup> and The Odin Team

**Abstract.** The water vapor line at 557 GHz was observed on November 8, 2002, with the Odin space telescope. The analysis of this observation, characterized by a high signal-to-noise ratio and a high spectral resolution, seems to favor a cometary origin (Shoemaker-Levy 9) for water in the stratosphere of Jupiter, in agreement with the ISO observation results.

### 1 Introduction

The Infrared Space Observatory has detected water vapor in the stratospheres of the giant planets and Titan as well as CO<sub>2</sub> on Jupiter, Saturn and Neptune (Feuchtgruber et al. 1997; Feuchtgruber et al. 1999; Lellouch 1999). The presence of the atmospheric cold trap implies an external origin for H<sub>2</sub>O, which could be the permanent infall of interplanetary dust particles (IDP), the sputtering from the rings and/or satellites or the impact of kilometer-sized comets. In the case of Jupiter, the sources of water could either be IDP (Bergin et al. 2000) or the Shoemaker-Levy 9 (SL9) comet impacts in 1994 (Lellouch et al. 2002).

The submillimeter satellite Odin has been launched in 2001 and carries out a long lasting monitoring of Jupiter's water vapor line (110-101) at 557 GHz. As an example, the high resolution H<sub>2</sub>O spectrum obtained on November 8<sup>th</sup> 2002 is presented and discussed here. Both the IDP and the SL9 origins have been modeled with our photochemical model (Ollivier et al. 2000, adapted to Jupiter).

A description of the observations is given in Sect. 2. Our photochemical and radiative transfer models are briefly described in Sect. 3. Some preliminary results are presented in Sect. 4.

### 2 Observations

The Odin space telescope detected the water vapor 557 GHz line on Jupiter in November 2002. The resulting brightness temperature spectra have a high signal-to-noise ratio ( $\sim 12$ ). The spectral band is 1 GHz and the spectral resolution is about 1 MHz.

The Odin observations were carried out with the Acousto-Optical Spectrometer (AOS) in a classical position switching mode. As Jupiter has a strong continuum emission at this frequency, stationary waves are generated within the instrument, causing ripples on the spectrum (Fig. 1). The subtraction of the ripple is the source of an uncertainty of 10% on the line contrast and some uncertainty on the line wing shape.

---

<sup>1</sup> Université Bordeaux 1, CNRS, OASU, LAB, 2 rue de l'Observatoire, 33270 Floirac, France

<sup>2</sup> (the same as T. Cavalié listed above)

<sup>3</sup> LESIA, Observatoire de Paris, France

<sup>4</sup> (the same as E. Lellouch listed above)

<sup>5</sup> (the same as T. Cavalié listed above)

<sup>6</sup> (the same as T. Cavalié listed above)

<sup>7</sup> (the same as E. Lellouch listed above)

<sup>8</sup> Onsala Space Observatory, Sweden

<sup>9</sup> Stockholm Observatory, Sweden

<sup>10</sup> Swedish Space Corporation, Sweden

<sup>11</sup> (the same as A. Hjalmarson listed above)

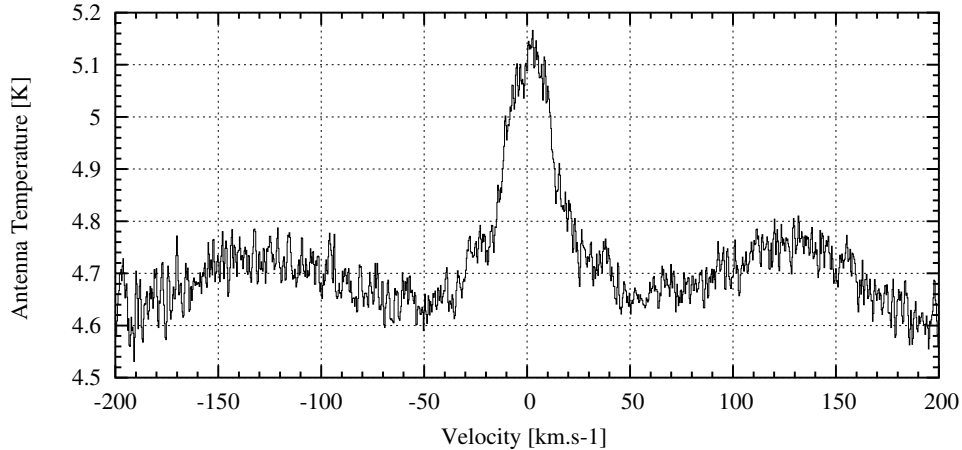


**Fig. 1.** Odin observations of Jupiter at the H<sub>2</sub>O (110-101) line frequency of November 8, 2002. The observed antenna temperature is displayed as a function of velocity.

All the observed features correspond to the emission of the whole planet as the beam size (2.1' for Odin) is greater than the planet size ( $\sim 35\text{-}40''$ ). The line width is almost entirely due to the smearing effect because of limb equatorial velocity  $\sim 12.6 \text{ km.s}^{-1}$  of the planet (Bergin et al. 2000). As no absolute calibration has been done, all results are discussed in terms of line-to-continuum ratios.

### 3 Modeling

We performed our data analysis in three steps: first, we used our photochemical code to provide a water vapor vertical profile and then used this profile to compute the resulting spectral line. Finally, comparing the synthetic spectrum with the data allowed us to fix the input parameters of the photochemical code (input of water vapor).

#### 3.1 Photochemical modeling

We used a time-dependant photochemical model, which derives from the model established for Saturn by Ollivier et al. (2000) and which has been adapted to the case of the atmosphere of Jupiter. For each altitude and each chemical compound  $i$ , the continuity equation (3.1) is solved.

$$\frac{dn_i}{dt} = P_i - n_i L_i - \text{div}(\phi_i) \quad (3.1)$$

$n$  is the concentration,  $P$  the chemical production,  $L$  the chemical loss and  $\phi$  the vertical flux. This is a one dimension model since only the vertical transport is considered.

The model includes 46 oxygen compounds and hydrocarbons and 593 reactions (photolysis processes and chemical reactions). Condensation near the tropopause is also considered. The eddy diffusion coefficient profile we took comes from Moses et al. (2005). We chose their nominal eddy profile called "model C".

Feuchtgruber et al. (1997) and Moses et al. (2000) showed that an IDP source is more likely than a ring/satellite source since there is a difference of two orders of magnitude in the estimated fluxes. This is the reason why we chose to compare the results of two models: an IDP source model and a IDP+SL9 source model. The lack of spatial resolution of the observations allowed us to use disk-averaged abundance vertical profiles for water, even if the SL9 impacts were all located in the southern hemisphere. The only input parameter we had to fix to test the IDP source hypothesis is the external flux of infalling water  $\Phi_{\text{H}_2\text{O}}^{\text{IDP}}$ . In order to test the SL9 source hypothesis, we have built vertical profiles at the time of the impacts (July 1994) and let them evolve with the photochemical model until the time of the observations (November 2002 for the Odin data). The initial water vertical profiles have been built on the base of a low stationary external flux and a sporadic external flux, due to the comet. The low stationary input flux is modeled via an IDP model with a flux  $\Phi_{\text{H}_2\text{O}}^{\text{IDP}} = 4 \cdot 10^4 \text{ cm}^{-2}\text{s}^{-1}$  (Lelluch et al. 2002). This value is 2 orders of magnitude lower than a pure IDP model (see Sect. 4).

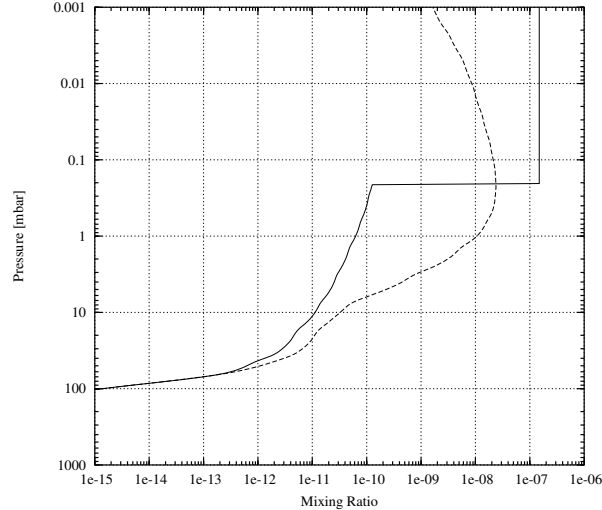


**Fig. 2.** SL9 source vertical profiles of water at the time of the SL9 impacts (07/1994) in solid line and at the time of the Odin observations (11/2002) in dashed lines. The evolution of water abundance is computed by the photochemical model. The water vapor mixing ratio is displayed as a function of atmospheric pressure. Profiles correspond to a fixed value of  $p_0=0.2$  mbar, and an adjusted value of  $q_0=1.5 \cdot 10^{-7}$

The sporadic input of water due to the impacts was modeled via two parameters: the deposition pressure  $p_0$  and the initial mixing ratio  $q_0$  above the  $p_0$  level (see Lellouch et al. 2002 for more details). The value of  $q_0$  was set to a constant value.

Thus, we have two possibilities for the SL9 models. The first one consists in fixing the value of  $p_0$  and adjusting the value of  $q_0$  with the data. In the second case, we fix  $q_0$  and adjust  $p_0$ . Some constraints exist on both  $p_0$  and  $q_0$ . The most reliable constrain is probably the fact that the deposition level that was observed for CO during the SL9 impacts is  $0.2 \pm 0.1$  mbar (Moreno 1998). The other constrain lies on the observed column density of water vapor. Lellouch et al. 2002 inferred that the  $\text{H}_2\text{O}/\text{CO}$  ratio is equal to 0.07 in mass to explain the entire ISO data set, thus fixing the  $\text{H}_2\text{O}$  column density to  $(2.0 \pm 0.5) \cdot 10^{15} \text{ cm}^{-2}$ . We kept these numbers in mind in order to constrain our SL9 source models. An example when fixing  $p_0$  is shown on Fig. 2 as well as the profile, at the time of the observations, computed by the photochemical model.

### 3.2 Radiative transfer modeling

We modeled the observed submillimetric radiations with a line-by-line non-scattering radiative transfer model. We computed synthetic spectra of the  $\text{H}_2\text{O}$  557 GHz line. The program respects the approximate spherical geometry of the planet so that planetary disk and limb contributions are taken into account. We assumed an uniform distribution of all other opacity sources and we adopted mean thermal profile of the atmosphere of Jupiter (Fouchet et al. 2000a) since our beam size is larger than the observed planetary disk. Continuum opacity is dominated by  $\text{H}_2$ -He- $\text{CH}_4$  collision-induced absorption (Borysow et al. 1985, 1986 and 1988). Following Moreno (1998), the opacity due to the far wings of ammonia and phosphine lines was also included. We used the Fouchet et al. (2000b) ammonia and phosphine mixing ratio vertical profiles. Spectroscopic parameters for  $\text{NH}_3$ ,  $\text{PH}_3$  and  $\text{H}_2\text{O}$  were taken from Pickett et al. (1998).

The rapid rotation of Jupiter (9.9 h) induces the smearing of the disk-averaged line on the spectrum, because of the Doppler shifts due to the gas rotation velocity ( $12.6 \text{ km}\cdot\text{s}^{-1}$  at the eastern and western limbs). The way this effect is taken into account is described in Bergin et al. (2000).

## 4 Preliminary results

The best fit models we obtained are displayed in Fig. 3. We derived an external flux of water, originating from an IDP source, of  $\Phi_{\text{H}_2\text{O}}^{\text{IDP}}=4.5 \cdot 10^6 \text{ cm}^{-2}\text{s}^{-1}$ . This value is greater than the one derived by Bergin et al. (2000) by a factor of less than 2. Nevertheless, their model did only include vertical transport (no chemical processes).

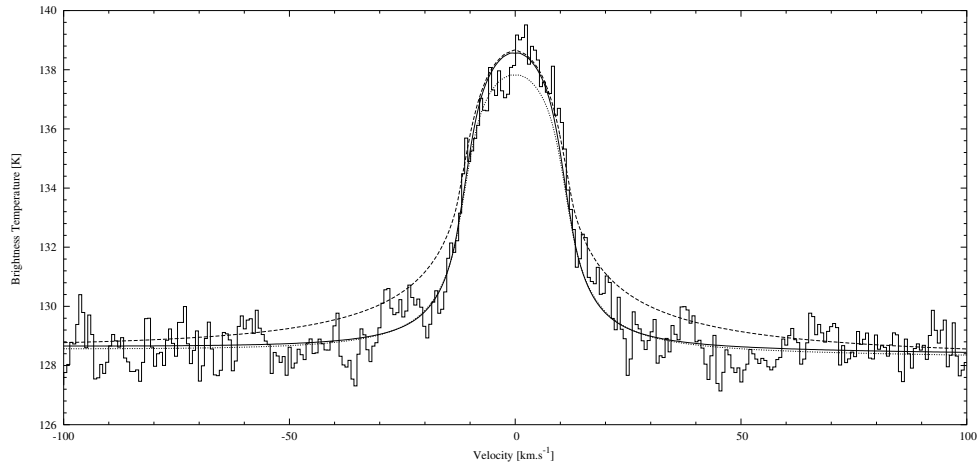


**Fig. 3.** Brightness temperature spectrum of Jupiter at 557 GHz with the best fit models for each external origin hypothesis. The IDP source fit (dashed lines) results in too broad wings compared to both SL9 source fits. The dotted lines corresponds to the couple of parameters ( $p_0=0.45$  mbar;  $q_0=6 \cdot 10^{-8}$ ) and the solid line to the couple ( $p_0=0.2$  mbar;  $q_0=1.5 \cdot 10^{-7}$ ).

Taking photolysis and chemical losses into account, they would probably have obtained a higher value for the flux consistent with our result. When considering the SL9 source hypothesis and fixing the value of  $q_0$  at  $6 \cdot 10^{-8}$ , we derive a deposition pressure level  $p_0$  of 0.45 mbar. When fixing  $p_0=0.2$  mbar, we obtain  $q_0=1.5 \cdot 10^{-7}$ , leading to a water column density of  $2.6 \cdot 10^{15} \text{ cm}^{-2}$ . The latter set of parameters better reproduces the line contrast than the previous one (see Fig. 3).

The overall best fit model is the SL9 source model with  $p_0=0.2$  mbar. The line wings are better modeled with such a model than with an IDP source model, which gives too broad wings. Moreover, the model satisfies the constraints derived from CO deposition observations and is close to the  $\text{H}_2\text{O}$  column density as measured by ISO.

This result tends to confirm the ISO conclusions on the origin of water in the stratosphere of Jupiter. However, these results must be confirmed by re-analysing the SWAS data with the same model and trying to reproduce the ISO lines as well. Though, the signal to noise ratio is insufficient to firmly conclude in favor of the SL9 source when only considering the Odin data. Further observations with Odin as well as observations with Herschel would be very valuable with regards to answering the question of the origin of water in the stratosphere of Jupiter.

## References

- Bergin, E.A., Lellouch, E., Harwit, M., et al. 2000, *ApJ*, 539, L147  
 Borysow, J., Trafton, L., Frommhold, L., et al. 1985, *ApJ*, 296, 644  
 Borysow, A., Frommhold, L., 1986, *ApJ*, 304, 849  
 Borysow, J., Frommhold, L., & Birnbaum, G., 1988, *ApJ*, 326, 509  
 Feuchtgruber, H., Lellouch, E., de Graauw, T., et al. 1997, *Nat*, 389, 159  
 Feuchtgruber, H., Lellouch, E., Encrenaz, T., et al. 1999, *The Universe as Seen by ISO*, Eds., P.Cox & M.F. Kessler, ESA-SP, 427, 133  
 Frisk, U., Hagström, M., Ala-Laurinaho, J., et al. 2003, *A&A*, 402, L27  
 Fouchet, T., Lellouch, E., Bézard, B., et al. 2000a, *A&A*, 355, L13  
 Fouchet, T., Lellouch, E., Bézard, B., et al. 2000b, *Icarus*, 143, 223  
 Lellouch, E., 1999, *The Universe as Seen by ISO*, Eds., P.Cox & M.F. Kessler, ESA-SP, 427, 125  
 Lellouch, E., Bézard, B., Moses, J.I., et al. 2002, *Icarus*, 159, 112  
 Ollivier, J.-L., Dobrijevic, M., & Parisot, J.-P., 2000, *Planet. Space Sci.*, 48, 699  
 Pickett, H.M., Poynter, R.L., Cohen, E.A., et al. 1998, *J. Quant. Spectrosc. & Rad. Transfer*, 60, 883

Moreno, R., 1998, PhD Thesis, Université Paris VI

Moses, J.I., Bézard, B., Lellouch, E., et al. 2000, *Icarus*, 145, 166

Moses, J.I., Fouchet, T., Bézard, B., et al. 2005, *J. Geophys. Res.*, 110, E08001